Materials Characterization 138 (2018) 255–262

Contents lists available at ScienceDirect

Materials Characterization

journal homepage: www.elsevier.com/locate/matchar

Microstructure and fracture properties of open-cell porous Ti-6Al-4V with high porosity fabricated by electron beam melting

S.Y. Chen[a], C.N. Kuo[b,c,d,*], Y.L. Su[d,e], J.C. Huang[a,f,**], Y.C. Wu[a], Y.H. Lin[a], Y.C. Chung[a], C.H. Ng[a]

[a] Department of Materials and Optoelectronic Science, National Sun Yat-Sen University, Kaohsiung 80424, Taiwan, ROC
[b] Department of Bioinformatics and Medical Engineering, Asia University, Taichung 41354, Taiwan, ROC
[c] 3D Printing Medical Research Institute, Asia University, Taichung 41354, Taiwan, ROC
[d] Casting Technology Section, Metal Processing R&D Department, Metal Industries Research & Development Centre, Kaohsiung 81160, Taiwan, ROC
[e] 3D Printing Medical Research Center, China Medical University Hospital, Taichung 40447, Taiwan, ROC
[f] Institute for Advanced Study, Department of Materials Science and Engineering, City University of Hong Kong, Kowloon, Hong Kong

ARTICLE INFO

Keywords:
Electron beam
Ti alloy
Porosity
Mechanical property
Additive manufacturing

ABSTRACT

The open-cell porous Ti-6Al-4V structure with high porosity, intended to be applied as replacement for human cancellous bone, were fabricated by electron beam melting (EBM). Computer aided design (CAD) was applied to design porous structures using the same unit cell with different unit cell sizes from 2.5 to 4 mm, different ligament widths from 600 to 900 μm, and different pore sizes from 1200 to 1800 μm, in order to achieve high porosity of 80% in avoiding the stress shielding effect. In comparison with the CAD designs and the EBM samples, there were minor discrepancies in terms of pore size and ligament width, mainly a result of melting pool. The measured data on the Young's modulus and yield strength of the EBM porous samples can be predicted by the Gibson and Ashby model. All samples with high porosity were found to match well with cancellous bone, with Young's modulus of 2 GPa and yield stress of 31 MPa, effective to diminish the risk of stress shielding effect. For porous EBM sample with high 80% porosity, the work of fracture can increase from 15.9 to 47.6 kJ/m^2 with increasing ligament width from 600 to 900 μm.

1. Introduction

Additive manufacturing (AM), or called as rapid prototyping or 3D printing, fabricating materials directly into the final 3D shape, has become more and more popular in recent years. AM technologies can be classified as different methods according to the input raw materials [1]. For metal powder materials, the most popular 3D printing technology is powder bed fusion (PBF). The products can be fabricated by melting metal powders layer by layer to build up each thin cross-sections of the product sliced from the original computer aided design (CAD) data [2]. Electron beam melting (EBM) and selective laser melting (SLM) processes have been developed successfully for metal part by melting metal powders together using different melting sources of electron beam or laser beam [3]. Due to the nature of electron and laser beams, the density of the resulting parts fabricated by EBM can usually be higher than those built by SLM [3,4].

Among many kinds of metal materials applied for biomedical implants, Ti-based alloys exhibit good mechanical, physical and biological properties. And thus Ti-based alloys, especially Ti-6Al-4V, are the commercially preferred candidates for hard tissue replacement applications such like bone implants [5]. However, the Young's modulus of Ti-based alloys (100–140 GPa) [6] is still much higher than the Young's modulus of human's cortical and trabecular bone (1–30 GPa) [7,8]. The modulus difference between metal implants and bone tissue will make the implant basically sustain the load alone which would inevitably lead to bone osteoporosis, called as the stress shielding effect [9].

According to the Gibson and Ashby model [10], the mechanical properties including elastic modulus and yield stress are related to the porosity (or the relative density) of porous materials. Hence, applying porous structures could be the solution to reduce the modulus difference between Ti-based parts and human bones. There have been numerous studies investigating the mechanical properties of porous implants fabricated by AM SLM [11–14]. Our previous study [14] using SLM to prepare the Ti-4Al-6V foams, give the following relationship

$$E/E_s = 1.5(\rho/\rho_s)^2 \quad (1)$$

$$\sigma_{pl}/\sigma_s = 1.1(\rho/\rho_s)^{1.5}, \quad (2)$$

* Correspondence to: C.N. Kuo, Department of Bioinformatics and Medical Engineering, Asia University, Taichung 41354, Taiwan, ROC.
** Correspondence to: J.C. Huang, National Sun Yat-Sen University, 70 Lienhai Rd., Kaohsiung 80424, Taiwan, ROC.
E-mail addresses: cnkuo@asia.edu.tw (C.N. Kuo), jacobc@mail.nsysu.edu.tw, chihuang@cityu.edu.hk (J.C. Huang).

https://doi.org/10.1016/j.matchar.2018.02.016
Received 20 October 2017; Received in revised form 25 January 2018; Accepted 13 February 2018
Available online 16 February 2018

where E is the elastic modulus of the porous structure, E_s is the elastic modulus of the open-cell edge (ligament) material, σ_{pl} is the plateau stress of the porous material, σ_s is the yield strength of the ligament material, ρ is the porous structure density, ρ_s is the density of the ligament material. The elastic modulus (E_s) and yield strength (σ_s) for dense solid Ti-6Al-4V alloys fabricated by SLM are 110 GPa and 990 MPa [15]. But it was found that SLM foams with higher porosity greater than 60% tend to possess lower modulus and stress than those predicted by Eqs. (1) and (2). The ligaments bonded during SLM, in foams with high porosity levels from 60% to 80% or above, were seen to be weaker than expectation.

The high porosity of porous structures could not only avoid the stress shielding effect but also improve the bone ingrowth effect by introducing sub-millimeter-sized pores [16]. Compared with SLM, the EBM process could cause stair steps to induce a larger surface roughness on the dense solid samples [17]. For bionic implants, the surface roughness could sensitively affect the bone cell attachment performance of the implants, claimed to increase with increasing the surface roughness [18]. On the other hand, in terms of mechanical property, the rougher surface could induce stress concentrations so to reduce the fatigue life of porous materials fabricated by AM process [19]. Both the bone cell attachment and mechanical performance need to be considered and balanced.

In literature, there are still few studies focusing on relationship between surface roughness and fracture properties of high porosity materials, especially for the AM EBM foams. In this study, this relationship is systematically examined and rationalized for the EBM prepared Ti-6Al-4V foams with high porosity.

2. Materials and Methods

The pre-alloyed Ti-6Al-4V powders (Titanium Ti64ELI) were purchased from Arcam, Sweden. The AM EBM process was conducted by Arcam Q10 system which was developed as the 3rd generation EBM technology. The Ti-6Al-4V EBM specimens were fabricated using He protective atmosphere at 1×10^{-3} Torr, with an input EB gun voltage and current of about 40 kV and 15–17 mA, scanning speed of 4500 mm/s, spot size of 100 μm, and each metal powder layer thickness of 50 μm. Using Materialise Magics[19] CAD software, the CAD models of open-cell porous samples were designed and built in with different unit cell sizes based on type of diamond unit cell, fabricated to porous cylinders with a diameter of 10 mm and a height of 20 mm, as shown in Fig. 1.

The microstructure nature of raw powders and EBM porous foams were examined by X-ray diffraction (SIEMENS D5000 X-ray diffractometer (XRD)). The voltage and current of XRD using the Cu-Kα radiation with wavelength of 1.5406 Å were 40 kV and 30 mA, equipped with 0.02 mm graphite monochrometer. The range of diffraction angle 2θ was set from 20° to 80° at a scanning rate of 0.05° per four seconds. In order to observe the microstructure and morphology of the powders and porous structures, scanning electron microscopy (SEM, JEOL JSM-6330) combined with the quantitative image analysis software, ImageJ, was applied. The size distribution of starting powders was characterized by Mastersizer 2000 from Malvern, England. In addition, the ligament surface roughness and fracture properties were analyzed using a Zeiss Metrotom 800 Micro computed tomography (micro-CT) using a voltage of 100 kV and a power of 15 W.

The EBM cylindrical porous samples were subject to compression testing, with a strain rate of $1 \times 10^{-4}\,s^{-1}$ at room temperature by using the Instron 5582 universal testing machine. In order to increase the accuracy of strain, all compression tests were conducted equipped with the Instron 2601 Linear Variable Differential Transformer (LVDT) displacement transducer. All compression tests have been conducted for at least 3 times, and the averages are presented.

3. Results and Discussion

The as-received Ti-6Al-4V powders practically appear smooth, spherical, fully dense and sometimes with a few non-spherical powders, as shown in Fig. 2(a). Using the image analysis software ImageJ, the circularity of the Ti-6Al-4V powders is about 0.962 ± 0.024, which is considered to be high circularity beneficial for powder flow during AM EBM [20]. The average powder size (d_{50}) is 75.1 ± 0.8 μm, determined from the particle size distribution shown in Fig. 2(b) measured by the particle size analyzer (Mastersizer 2000).

The commercial Ti-6Al-4V alloys typically contain hexagonal closed packing (HCP) α phase stabilizer (Al) and body-centered cubic (BCC) β phase stabilizer (V). It is well-known that the metallurgical phases present in an alloy can be controlled by different heat treatment temperatures and cooling rates. When the processing of Ti-6Al-4V is conducted with a low cooling rate, the α phase begins to form below the β transformation temperature, which is about 980 °C [21,22]. However, Ahmed and Rock [23] had investigated that Ti-6Al-4V samples would possess fully martensitic α′ phase when the melt was exposed to cooling rates above 410 °C/s. According to JCPDS file #44-1288, the β-Ti phase

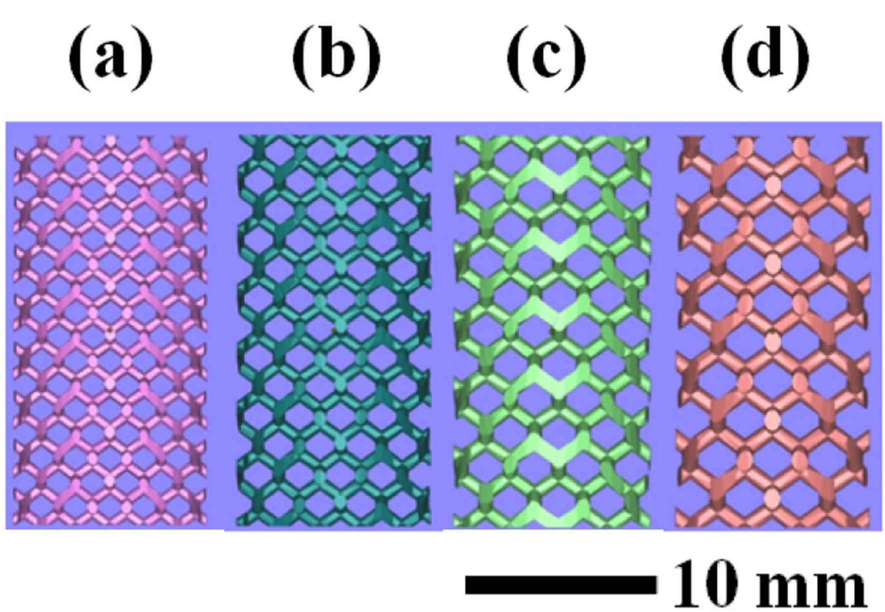

Fig. 1. The CAD data with different unit cell sizes of the open-cellular structures: (a) 2.5 mm, (b) 3 mm, (c) 3.5 mm and (d) 4 mm.